FIRST ORDER DIFFERENTIAL MICROPHONE ARRAYS FOR AUTOMOTIVE APPLICATIONS

Markus Buck, Martin Rößler

TEMIC speech processing
Soeflinger Strasse 100, 89077 Ulm, Germany
`markus.buck@temic.com`, `martin.roessler@temic.com`

ABSTRACT

Differential microphone arrays promise high directional gain with compact arrangements. However, they also come with the problem that even small deviations in microphone properties can cause severe degradation of the array's performance. For automotive applications the effects of microphone deviations have to be reduced. In this paper the performance of first order differential arrays is examined. The frequency dependence of the important parameters is thoroughly investigated. This paper contributes the expression for the frequency dependent directivity index, which is published for the first time for differential arrays. Furthermore a new approach to model effects of microphone deviations for low frequencies is presented.

1. INTRODUCTION

A differential microphone array consists of two omni-directional sensors with distance d as shown in Fig. 1. Sound from endfire direction $\theta = 0$ takes the acoustic delay $\tau_A = \frac{d}{c}$ between the sensors. With the delay τ ($0 \leq \tau \leq \tau_A$) the directivity pattern can be adjusted. The direction of arrival of the desired signal is always $\theta = 0$ for a differential array.
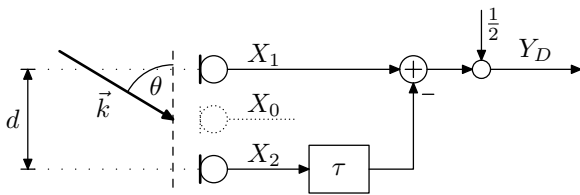
Figure 1: Structure of a first order differential array.

2. DIRECTIONAL RESPONSE

The array is excited by plane waves with wavenumber $\vec{k}$. Because of radial symmetry the sensor signals $X_1(\omega)$ and $X_2(\omega)$ can be expressed with the angle of

incidence θ and the frequency ω. There is the relation $|\vec{k}|d = kd = \omega\tau_A$ between wavenumber and frequency.

At the center point of the array the signal $X_0(\omega)$ could be picked up by a virtual microphone. A plane wave impinging under angle θ with wavenumber $k = \frac{2\pi}{\lambda}$ evokes the microphone signals $X_1(\omega)$ and $X_2(\omega)$,

$$X_1(\omega) = X_0(\omega) \cdot \exp\{j\tfrac{kd}{2}\cos\theta\} , \qquad (1)$$

$$X_2(\omega) = X_0(\omega) \cdot \exp\{-j\tfrac{kd}{2}\cos\theta\} . \qquad (2)$$

The output of the differential array is

$$Y_D(\omega) = \tfrac{1}{2}\left(X_1(\omega) - X_2(\omega) \cdot \exp\{-j\omega\tau\}\right) . \qquad (3)$$

The directional response of the array H_D is the transfer function from the fictitious microphone signal $X_0(\omega)$ to the array output $Y_D(\omega)$,

$$H_D(\omega, \theta) = j \cdot \exp\{-j\tfrac{\omega\tau}{2}\} \cdot \sin\left(\tfrac{kd}{2}(\tfrac{\tau}{\tau_A} + \cos\theta)\right) . \quad (4)$$
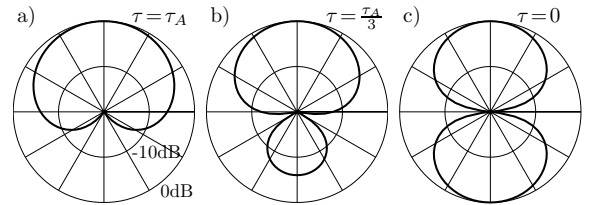
Figure 2: Shapes of the directivity pattern for low frequencies: (a) cardioid, (b) hypercardioid, (c) dipole

In literature usually very small distances $kd \ll 1$ are assumed which justify the approximation $\sin\alpha \approx \alpha$. In this case, there is an idealized directional response $\widetilde{H}_D$,

$$H_D(\omega, \theta) \approx \widetilde{H}_D(\omega, \theta) = j \cdot \tfrac{kd}{2} \cdot (\tfrac{\tau}{\tau_A} + \cos\theta) . \qquad (5)$$

In this representation, basic characteristics of differential arrays are obvious :

- The shape of $\widetilde{H}_D(\theta)$ is determined by $\frac{\tau}{\tau_A} + \cos\theta$ which is not dependent on frequency [5]. Well known shapes as the dipole ($\frac{\tau}{\tau_A} = 0$), the cardioid ($\frac{\tau}{\tau_A} = 1$) and the hypercardioid ($\frac{\tau}{\tau_A} = \frac{1}{3}$) are shown in Fig. 2.

- Due to the signal subtraction in Fig. 1 a phase shift of $\frac{\pi}{2}$ occurs.

- The directional response $\widetilde{H}_D(\omega)$ shows first order high pass characteristics (Fig. 3a).

For low frequencies the difference signal Y_D gets very susceptible to any disturbances because of the high pass characteristics of $H_D(\omega)$. Due to this reason, the distance d should not be chosen too small, what may conflict with the postulation $kd \ll 1$.

3. DEPENDENCE ON FREQUENCY

3.1. Cut-off-frequency

In the exact response (Eq. (4)) there is the sine function scaling the amplitude. It is only reasonable to operate the differential array in the low frequency range, up to the first maximum of the sinus. This first maximum fixes the cut-off-frequency ω_c,

$$\omega_c = \frac{\pi}{\tau_A + \tau} \; . \tag{6}$$

Fig. 3a shows the exact frequency response according to Eq. (4) for a cardioid. The cut-off-frequency is marked with a circle. For low frequencies the directional characteristics (first order gradient) are approximately independent of frequency. This is obvious because of the parallel lines in Fig. 3. However, as the frequency increases the shape gets more and more deformed. Even total cancellation of the desired signal occurs at certain frequencies.
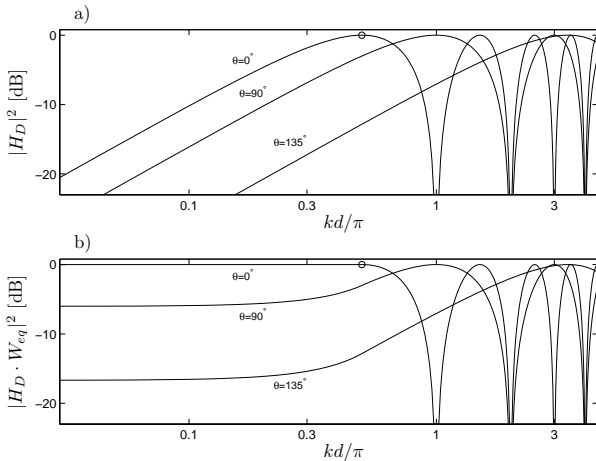
Figure 3: Directional response H_D of a cardioid for selected angles (a) without and (b) with equalization.

3.2. Equalization Filter

In order to compensate the highpass characteristics of $H_D(\omega, \theta)$ a filter $W_{eq}(\omega)$ has to be designed. For the endfire direction $\theta = 0$ the equalized frequency response $H_D(\omega, \theta = 0) \cdot W_{eq}(\omega)$ has to equal 0dB for frequencies below ω_c.

$$W_{eq}(\omega) = \begin{cases} \dfrac{1}{\sin(\frac{\pi}{2} \cdot \frac{\omega}{\omega_c})} & , 0 < \omega \leq \omega_c \\ 1 & , \text{otherwise} \end{cases} \tag{7}$$

The equalized directional response $H_D(\omega, \theta) \cdot W_{eq}(\omega)$ is shown in Fig. 3b.

For low frequencies $\omega \to 0$ the equalization filter W_{eq} assumes very high values. That means that any disturbance of the signals is strongly amplified. A lower limit for signal disturbance is represented by sensor noise. It determines the minimum limit for the frequency range that is reasonable for operation of a differential array. Any additional error sources such as microphone mismatch push the lower bound up to higher frequencies.

3.3. Directivity index

The array gain which is achieved in a spherical isotropic noise field defines the directivity index DI. It can be calculated by averaging the squared absolute value of the directional response over the whole sphere (geometric interpretation) [3].

$$DI(\omega) = \frac{|H(\omega, \theta = 0)|^2}{\frac{1}{4\pi} \int_0^{2\pi} \int_0^{\pi} |H(\omega, \theta)|^2 \sin\theta \, d\theta \, d\phi} \tag{8}$$

Taking the exact response H_D from Eq. (4) a new frequency dependent expression for the directivity index can be derived, where $\text{si}(x) = \frac{1}{x} \sin(x)$.

$$DI_D(\omega) = \frac{2 \cdot \sin^2\left(\frac{\omega}{2}(\tau_A + \tau)\right)}{1 - \text{si}(\omega\tau_A) \cdot \cos(\omega\tau)} \tag{9}$$
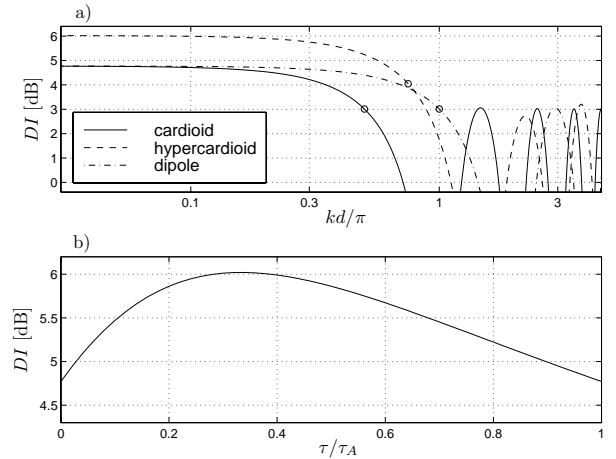
Figure 4: (a) DI for cardioid, hypercardioid and dipole. (b) DI for low frequencies, $kd \ll 1$.

The well known directivity index for low frequencies

$$\lim_{\omega \to 0} DI_D(\omega) = \widetilde{DI}_D = \frac{3(\tau_A + \tau)^2}{3\tau_A{}^2 + 3\tau^2} \tag{10}$$

is also the result for the approximated response $\widetilde{H}_D$ from Eq. (5). Fig. 4a shows the directivity index for the dipole, the cardioid and the hypercardioid. The cut-off-frequencies are marked with circles. The directivity index DI_D assumes even negative values for some frequencies above ω_c. Fig. 4b shows the directivity index for low frequencies according to Eq. (10). It is well known that the hypercardioid ($\frac{\tau}{\tau_A} = \frac{1}{3}$) maximizes the approximated directivity index $\widetilde{DI}_D$.

4. RELATION TO THE SUPERDIRECTIVE ENDFIRE ARRAY

A big disadvantage of differential arrays is the cleft curve of the DI for increasing frequencies. In the higher frequency range a simple delay and sum beamformer that is steered in endfire direction works better than the differential array. The idea is to combine the advantages of both structures: the high directional gain of the differential array at low frequencies and the roughly frequency independent gain of the delay and sum array for the upper frequency range.

The optimal structure for a microphone array with respect to the DI is the superdirectional beamformer (SDB). It can be realized by a delay and filter structure or equivalently by a GSC like structure with a fixed filter as shown in Fig. 5 [4]. This structure can be interpreted as a combination of an endfire delay and sum beamformer and a differential beamformer. The summation path contains the delay and sum signal Y_S. The difference path with signal $Y_D^{(i)}$ conforms with a cardioid differential array as shown in Fig. 1 however turned by 180°. The directional response of the delay
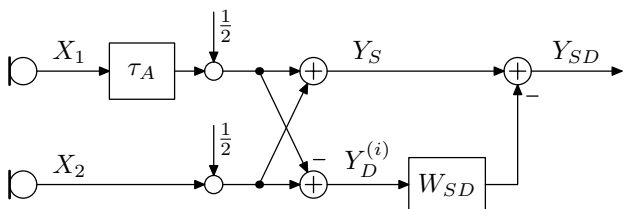
Figure 5: Structure of a superdirective array in GSC like form.

and sum beamformer $H_S(\omega, \theta)$ is

$$H_S(\omega, \theta) = \exp\{-j\tfrac{kd}{2}\} \cdot \cos\left(\tfrac{kd}{2}(1 - \cos\theta)\right) , \quad (11)$$

and the directional response of the turned cardioid is

$$H_D^{(i)}(\omega, \theta) = j \cdot \exp\{-j\tfrac{kd}{2}\} \cdot \sin\left(\tfrac{kd}{2}(1 - \cos\theta)\right) . \quad (12)$$

In both Eq. (11) and Eq. (12) all directional information lies in the term $\frac{kd}{2}(1 - \cos\theta)$. The basic difference between the sum and delay array and the differential array is the *cosine* and *sine* function that treat this directional term.

In order to achieve the optimum output signal Y_{SD}, the difference signal $Y_D^{(i)}$ has to be filtered by W_{SD} and then subtracted from the sum signal Y_S. The optimum filter is the Wiener solution [4]

$$W_{SD}(\omega) = \frac{-j \cdot \mathrm{si}(\omega\tau_A) \, \sin(\omega\tau_A)}{1 - \mathrm{si}(\omega\tau_A) \, \cos(\omega\tau_A)} . \quad (13)$$

It can be split into two parts. One part is the equalization filter $W_{eq}(\omega)$ for the differential array that is given in Eq. (7). The other part is a scaling filter $W_{sc}(\omega)$ that defines the weighting of the differential beamformer signal to the delay and sum beamformer signal.

$$W_{SD}(\omega) = -j \cdot W_{eq}(\omega) \cdot W_{sc}(\omega) \quad (14)$$

The scaling filter is shown in Fig. 6a. The directivity index for the endfire SDB [2] is known to be

$$DI_{SD}(\omega) = 2 \cdot \frac{1 - \mathrm{si}(2\,\omega\tau_A)}{1 - \mathrm{si}^2(\omega\tau_A)} . \quad (15)$$

At low frequencies the delay and sum path corresponds to an omnidirectional microphone and the differential path is approximately an ideal cardioid. With the weighting factor of $W_{sc} = 1.5$ the SDB output corresponds to a hypercardioid which is known to be optimum for the differential array. So the SDB operates as a differential array in the low frequency range. The directivity indices for the differential beamformer, the delay and sum beamformer and the SDB can be compared in Fig. 6b. Indeed the SDB assumes for low frequencies the same curve as the hypercardioid. Above the cut-off-frequency the delay and sum endfire beamformer outperforms the hypercardioid. But at any frequency the SDB takes the optimal value for the directivity index.
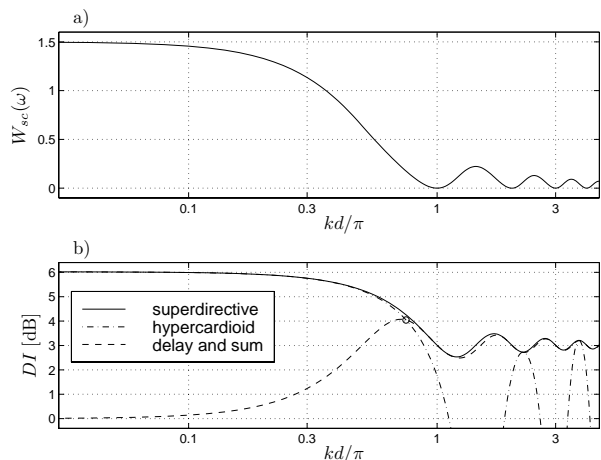
Figure 6: (a) Scaling filter $W_{sc}(\omega)$. (b) DI for SDB, hypercardioid and endfire delay and sum beamformer.

5. INFLUENCE OF MICROPHONE TOLERANCES

In this section the influence of microphone mismatch on first order differential arrays is investigated. A suitable model for microphone mismatch [1] consists of a transfer function $M = M_{\text{ref}} + \Delta M$. The nominal sensor transfer function M_{ref} is in this case normalized to the value 1. The deviation ΔM is assumed to be an independent random complex variable with $\sigma_M^2 = \mathcal{E}\{|\Delta M|^2\}$ where $\mathcal{E}\{.\}$ denotes the expectation value.

The signals of the two different sensors in Fig. 1 are

$$\widehat{X}_1(\omega) = X_0(\omega) \cdot (1 + \Delta M_1) \cdot \exp\{j\tfrac{kd}{2}\cos\theta\}, \quad (16)$$

$$\widehat{X}_2(\omega) = X_0(\omega) \cdot (1 + \Delta M_2) \cdot \exp\{-j\tfrac{kd}{2}\cos\theta\}. \quad (17)$$

The directional response $\widehat{H}_D$ for the differential array with microphone tolerances can be derived similar to Eq. (4). But now there are additional terms which depend on ΔM_i ($i = \{1,2\}$). Taking the expectation value of $|\widehat{H}_D(\omega,\theta)|^2$ the quadratic terms with $\mathcal{E}\{|\Delta M_i|^2\}$ remain whereas the linear terms $\mathcal{E}\{\Delta M_i\}$ disappear.

$$\mathcal{E}\{|\widehat{H}_D(\omega,\theta)|^2\} = |H_D(\omega,\theta)|^2 + 2\sigma_M^2 \qquad (18)$$

With this result a modified expression for the directivity index $\widehat{DI}_D(\omega)$ can be derived similar to Eq. (9).

$$\mathcal{E}\{\widehat{DI}_D(\omega)\} = \frac{2 \cdot \sin^2\left(\tfrac{\omega}{2}(\tau_A + \tau)\right) + \sigma_M^2}{1 - \text{si}(\omega\tau_A)\,\cos(\omega\tau) + \sigma_M^2} \qquad (19)$$

It is important to realize that in Eq. (18) the directional response $H_D(\omega,\theta)$ shows high pass characteristics. When the equalization filter W_{eq} from Eq. (7) is applied the effects of the microphone mismatch are strongly amplified for low frequencies.

6. EXPERIMENTAL RESULTS

A first order differential microphone array with variable distance d has been built up using microphones of the type Sennheiser ME102. Measurements in an anechoic chamber with plane waves from different angles of incidence θ yield the results shown in Fig. 7 where the directivity index has been derived from the measured directional response. In automotive applications it may be difficult to calibrate the microphones. For this reason the sensors have not been calibrated.

For a number of single microphones of the same type the frequency response has been measured. The average value of these responses has been taken as nominal frequency response M_{ref}. After normalization of the responses with respect to M_{ref} the variance of the microphone mismatch has been found to be $\sigma_M^2 = 0.038$. σ_M^2 is approximately independent of frequency and angle. Fig. 7 shows that the signal degradation for low frequencies is well predicted by the new model.
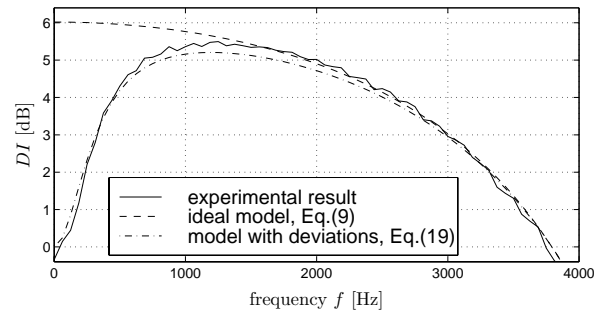
Figure 7: Experimental result for directivity index for a hypercardioid with $d = 5$cm.

7. CONCLUSIONS

In literature very little work can be found on the frequency dependent behaviour of differential arrays. This paper contributes the frequency dependent expression of the directivity index for first order differential microphone arrays. It can be extended by a model for microphone mismatch which predicts the behaviour at low frequencies.

With the new frequency dependent expression for the DI and the model for deviations, a frequency range can be determined for the favourable operation of the array. The lower bound of this range is set by the microphone properties such as deviations, the upper cut-off-frequency is set by the array geometry d. For automotive applications the distance d should not be chosen too small in order to increase robustness against sensor mismatch. Finally it is shown that the cut-off-frequency of the differential array can be overcome with a combination of a differential array and a delay and sum beamformer.

8. REFERENCES

[1] E. N. GILBERT AND S. P. MORGAN: *Optimum design of directive antenna arrays subject to random variables.* Bell System Technical Journal, vol. 34, pp. 637-663, 1955.

[2] H. COX ET AL.: *Robust adaptive beamforming.* IEEE Trans. on Acoustics, Speech and Signal Processing, vol. 35, pp. 1365-1375, 1987.

[3] G. W. ELKO: *Microphone array systems for hands-free telecommunication.* Speech Communication, vol. 20, pp. 229-240, 1996.

[4] J. BITZER ET AL.: *An alternative implementation of the superdirective beamformer.* Proc. 1999 IEEE Workshop on Applications of Signal Processing to Audio and Acoustics, New Paltz, New York, 1999.

[5] G. W. ELKO: *Superdirectional microphone arrays* in Acoustic Signal Processing for Telecommunication. Kluwer Academic, Dordrecht, 2000.